

A New Approach to Probing Minkowski Functionals

Dipak Munshi¹, Joseph Smidt², Asantha Cooray²

¹*School of Physics and Astronomy, Cardiff University, Queen's Buildings, 5 The Parade, Cardiff, CF24 3AA, UK*

²*Department of Physics and Astronomy, University of California, Irvine, CA 92697*

25 November 2010, Revision: 0.9

ABSTRACT

Most studies of Non-Gaussianity (NG) in the CMB data rely on moment based approaches that depend on the study of bispectrum or its higher order analogs of multispectra. In contrast, the studies that use the Minkowski functionals (MF) depend on morphological characteristics of the observed fields. The two approaches are complementary. Indeed, in a perturbative expansion of MFs, the lowest order terms correspond to the angular bispectrum albeit with a different set of weights for the individual modes. For all angular scales study of MFs are equivalent study of three one-point generalized skewness parameters. There has been lot of recent progress in estimation of skewness mainly through estimation of a spectrum associated with the ordinary skewness (namely the skew-spectrum). We show how the topological statistics such as MFs can also be computed from real data sets in the presence of mask and inhomogeneous noise by using methods for estimation of skew-spectrum. We exploit the fact that the computation of MF at the lowest order is equivalent to the estimation of three different skewness parameters. These one-point estimates are volume averages of third order statistics of fields that are constructed from the original data. Generalizing the concept of ordinary skew-spectra, which was recently introduced for the study of bispectrum, we define a sets of three different skew-spectra which specify the MFs at lowest order in non-Gaussianity and can probe them as a function of harmonic number. These spectra can also be studied independently to provide a valuable check for any cross-contamination from the secondaries or foreground sources. The Pseudo- C_l (PCL) approach is employed to estimate the generalized skew-spectra associated with the MFs in the presence of mask from noisy data. The variance for such estimators is analyzed. The results presented here are generic and can be useful in analyzing data from other projected surveys such as from the weak lensing surveys or from the future Sunyaev-Zel'dovich (SZ) surveys. Generalization to 3D can be done in a straight forward way which will be useful in quantifying the topology of galaxy distributions. We also go beyond the lowest order in skew-spectra and discuss the extraction of four generalized kurtosis and the corresponding kurt-spectra that are relevant in studying the next order corrections.

Key words: : Cosmology– CMB – Methods: analytical, statistical, numerical

1 INTRODUCTION

The study of Cosmic Microwave Background (CMB) radiation provides the cleanest window to probe the very early stages of the Universe's history. This can be used to probe the mechanism that generates seed perturbations which leads to the structure that we observe in the present day Universe. Recent observations by WMAP¹ supports the basic predictions of inflationary scenarios. It confirms that the primordial perturbations are nearly scale-invariant, adiabatic and nearly Gaussian. It is expected that the ongoing Planck² surveyor will improve our knowledge in these areas (see e.g. Tauber et al. (2010)).

It is well established now that non-Gaussianity from simplest inflationary models based on a single slowly-rolling scalar field is typically very small (Salopek & Bond 1990, 1991; Falk et al. 1993; Gangui et al. 1994; Acquaviva et al. 2003; Maldacena 2003), (see e.g. Bartolo, Matarrese & Riotto (2006) for a review). However there are many variants of simple inflationary models which include models with multiple scalar fields (Linde & Mukhanov 1997; Lyth, Ungarelli & Wands 2003), features in the inflationary potential, non-adiabatic fluctuations, non-standard kinetic terms, warm inflation (Gupta, Berera & Heavens 2002; Moss & Xiong 2007), or deviations from Bunch-Davies vacuum that can all lead to much higher level of non-Gaussianity.

Early observational work on the bispectrum from COBE (Komatsu et al. 2002) and MAXIMA (Santos et al. 2003) was followed by much more accurate analysis with WMAP (Komatsu et al. 2003; Creminelli et al. 2007; Spergel et al. 2007). With the recent claim of a detection of non-Gaussianity

¹ <http://map.gsfc.nasa.gov/>

² <http://www.rssd.esa.int/index.php?project=Planck>

(Yadav & Wandelt 2008) in the Wilkinson Microwave Anisotropy Probe 5-year (WMAP5) sky maps, interest in non-Gaussianity has obtained a tremendous boost. Much of the interest in primordial non-Gaussianity has focused on a phenomenological ‘local f_{NL} ’ parametrization in terms of the perturbative non-linear coupling in the primordial curvature perturbation (Verde et al. 2007):

$$\Phi(x) = \Phi_L(x) + f_{NL}(\Phi_L^2(x) - \langle \Phi_L^2(x) \rangle) + g_{NL}\Phi_L^3(x) + h_{NL}(\Phi_L^4(x) - 3\langle \Phi_L^2(x) \rangle^2) + \dots, \quad (1)$$

where $\Phi_L(x)$ denotes the linear Gaussian part of the Bardeen curvature and f_{NL}, g_{NL}, h_{NL} are the non-linear coupling parameters. A number of models have non-Gaussianity which can be approximated by this form. The leading order non-Gaussianity therefore is at the level of the bispectrum, or in configuration space at the three-point level. Many studies involving primordial non-Gaussianity have used the bispectrum, motivated by the fact that it contains all the information about f_{NL} (Babich 2005). It has been extensively studied (Komatsu, Spergel & Wandelt 2005; Creminelli 2003; Creminelli et al. 2006; Medeiros & Contaldi 2006; Cabella et al. 2006; Liguori et al. 2007; Smith, Senatore & Zaldarriaga 2009), with most of these measurements providing convolved estimates of the bispectrum. Optimized 3-point estimators were introduced by Heavens (1998), and have been successively developed (Komatsu, Spergel & Wandelt 2005; Creminelli et al. 2006; Creminelli, Senatore, & Zaldarriaga 2007; Smith, Zahn & Dore 2000; Smith & Zaldarriaga 2006) to the point where an estimator for f_{NL} which saturates the Cramer-Rao bound exists for partial sky coverage and inhomogeneous noise (Smith, Senatore & Zaldarriaga 2009). Approximate forms also exist for *equilateral* non-Gaussianity, which may arise in models with non-minimal Lagrangian with higher-derivative terms (Chen, Huang & Kachru 2006; Chen, Easther & Lim 2007). In these models, the largest signal comes from spherical harmonic modes with $\ell_1 \simeq \ell_2 \simeq \ell_3$, whereas for the local model, the signal is highest when one ℓ is much smaller than the other two – the so-called *squeezed* configuration.

While the bispectrum or its higher order analogs, multispectra, are more commonly used in studying departure from Gaussianity (Bartolo et al. 2004), alternative statistics such as Minkowski functional (MFs) too are routinely used for this purpose. MFs describe the morphological features of a fluctuating (random) fields Mecke, Buchert & Wagner (1994); Schmalzing & Buchert (1997); Schmalzing & Gořski (1998); Winitizki, Kosowsky (1998). The MFs for a Gaussian field is well understood and close form expressions exist (Tomita 1986). Any departure from the MFs of a Gaussian field will signify detection of non-Gaussianity. The MFs have been used to detect non-Gaussianity using projected (2D) fields such as CMB (Hikage et al. 2006), Weak Lensing (Matsubara & Jain 2001) as well as using 3D density fields as mapped by the Galaxy surveys e.g. SDSS (Park et al. 2005; Hikage et al. 2008, 2006; Hikage, Taruya & Suto 2003; Hikage et al. 2002). Several analytical results exist for prescriptions to model non-linear gravity as well as biasing schemes both in quasilinear and highly nonlinear regimes (Hikage et al. 2008). The MFs have been used also for the study of CMB data e.g. BOOMERanG data Natoli et al. (2010) as well as for the WMAP data (Komatsu et al. 2003; Eriksen et al. 2004). The MF based approach has also been used to study the effect of lensing on the CMB (Schmalzing, Takada & Futamase 2000).

While the study of primordial NG may be the primary motivation behind the study of MFs in the context of CMB, they have also been applied to probe gravity induced secondary NG using weak-lensing convergence or κ -maps Matsubara & Jain (2001); Taruya et al. (2002).

One of the main motivations behind studying various alternatives that probe primordial non-Gaussianity has to do with issues related to estimation. Different probes are affected differently by different contamination such as presence of foreground or say secondary non-Gaussianity. The methods based on multispectra that are typically employed for the estimation of non-Gaussianity typically employ a Fourier (or harmonic) space based approach. On the other hand, the techniques developed for estimation of MFs are traditionally employed in real space. Previously there has been many attempts to probe primordial non-Gaussianity using MFs (see e.g. Novikov (2000)). (Matsubara 2003) obtained a closed form expression for MFs in D dimension using a preservative expansion in terms of various orders of multispectra. At the lowest order, a departure from Gaussianity is characterized by three different skewness parameters $S^{(0)}, S^{(1)}, S^{(2)}$. The skewness parameter $S^{(0)}$ is the ordinary skewness that is most commonly used in various studies of non-Gaussianity for projected surveys as well as in 3D. The other set of skewness parameters are defined in terms of different cubic statistics that are constructed from the original data using differential operators.

This paper is organized as follows. In §2 we review the formalism of Minkowski Functionals. In §3 we focus on the one-point estimators, the generalized skewness and their links to Minkowski Functionals. In §3 we also introduce the concept of generalized skew-spectra and show how a power spectra can be defined for each of the Minkowski Functionals. In §4 the corrections to the lowest order in non-Gaussianity are discussed. These corrections are related to estimation of trispectra. In §5 real-life issues such as the mask and noise are discussed and estimators are designed for estimation of the Minkowski Functionals using a PCL based approach. In §6 we specialize the general discussion for the CMB sky. Various early Universe models and their predictions for the lower order multispectra are presented. Finally, §7 is left for discussion.

Throughout in this paper a WMAP7 (Larson et al. 2010) background cosmology will be used for computation of various spectra. The values of the parameters f_{NL}^{loc} and f_{NL}^{equi} , to be defined later, are set to unity. Some of the results developed here will have wider applicability, e.g. in the context of weak lensing surveys or projected galaxy surveys. Detailed results will be presented elsewhere. Results of implementation of our method on WMAP7 will be presented in an accompanying paper. The techniques developed here can also be applied for the study of SZ maps from future surveys.

2 FORMALISM

The MFs are well known morphological descriptors which are used in the study of random fields. Morphological properties are the properties that remain invariant under rotation and translation (see Hadwiger (1959) for more formal introduction). They are defined over an excursion set Σ for a given threshold ν . The three MFs that are defined for two dimensional (2D) studies can be expressed as:

$$V_0(\nu) = \int_{\Sigma} da; \quad V_1(\nu) = \frac{1}{4} \int_{\partial\Sigma} dl; \quad V_2(\nu) = \frac{1}{2\pi} \int_{\partial\Sigma} \kappa dl \quad (2)$$

Here da, dl are the elements for the excursion set Σ and its boundary $\partial\Sigma$. The MFs $V_k(\nu)$ correspond to the area of the excursion set Σ , the length of its boundary $\partial\Sigma$ as well as the integral curvature along its boundary which is related to the genus g and hence the Euler characteristics χ .

In our analysis we will consider a smoothed random field $\Psi(\hat{\Omega})$ with mean $\langle \Psi(\hat{\Omega}) \rangle = 0$ and variance $\sigma_0^2 = \langle \Psi^2(\hat{\Omega}) \rangle$. For a generic 2D weakly non-Gaussian random field Ψ on the surface of the sky. The spherical harmonic decomposition using $Y_{lm}(\hat{\Omega})$ as a basis function $\Psi(\hat{\Omega}) = \sum_{lm} \Psi_{lm} Y_{lm}(\hat{\Omega})$

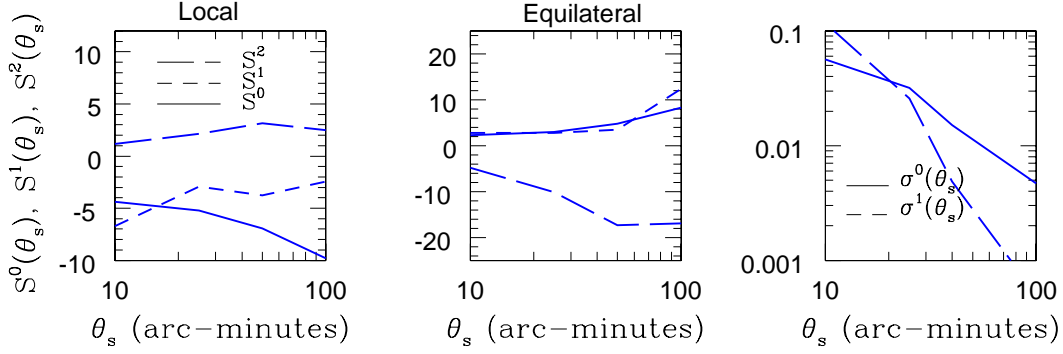


Figure 1. In the left and middle panel we display the One point third order statistics, i.e. the three skewness parameters $S^i(\theta_s)$ as a function of the beam FWHM θ_s . The left panel correspond to the *local* model of primordial non-Gaussianity and the middle panel depicts the *equilateral* model. In the right panel, the second order one-point parameters σ_0 and σ_1 as defined in Eq.(4) are plotted as a function of the beam FWHM. A WMAP7 background cosmology is assumed. Various plots in each panel correspond to the different FWHM as indicated. We consider four different beams with FWHM $\theta_s = 10', 25', 50', 100'$. Note that, being second order in nature, the parameters σ_i do not depend on the modeling of the bispectrum, which is a third order statistics. They depend only on the beam b_l and the underlying power spectra C_l . They are used in normalization of the skew- and kurt-spectra.

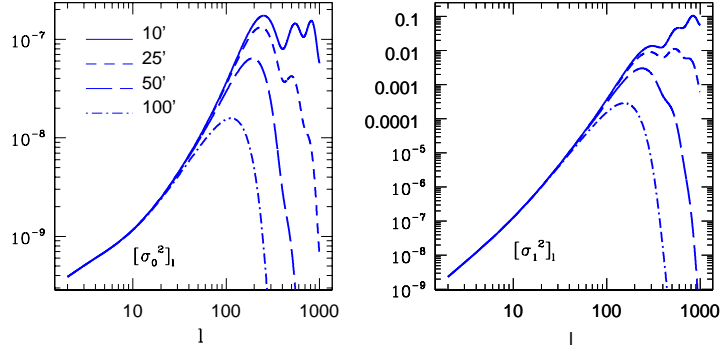


Figure 2. The contributions to the second order one-point parameters $[\sigma_0^2]_l$ and $[\sigma_1^2]_l$ as defined in Eq.(4) are plotted as a function of the harmonics l ; here $\sigma_i^2 = \sum_l (2l+1)[\sigma_i^2]_l$. A WMAP7 background cosmology is assumed for this calculation. Various plots represent different FWHM as indicated. We consider four different beams $\theta_s = 10', 25', 50', 100'$. Being two-point objects, these parameters do not depend on the modeling of the bispectrum and depend only on the experimental beam b_l and the underlying power spectra C_l . They are used in normalization while constructing the three different skew-spectra.

can be used to define the power spectrum C_l which is sufficient characterization of a Gaussian field $\langle \Psi_{lm} \Psi_{l'm'} \rangle = C_l \delta_{ll'} \delta_{mm'}$. For a non-Gaussian field the higher order statistics such as bi- or tri-spectrum can describe the resulting mode-mode coupling. Alternatively the topological measures such as Minkowski functionals which include Euler characteristics or genus can be employed to quantify deviation from Gaussianity. Indeed it can be shown that the information content in both descriptions are equivalent. At the leading order the MFs can be constructed completely from the knowledge of the bispectrum alone. We will be studying the MFs defined over the surface of the celestial sphere but equivalent results can be obtained in 3D using Fourier decomposition (Munshi 2010, in preparation). The MFs for a random Gaussian field is well known and is given by Tomita's formula (Tomita 1986). The notations and analytical results in this section are being kept generic however they will be specialized to the case of CMB sky in subsequent discussions. The MFs denoted as $V_k(\nu)$ for a threshold $\nu = \Psi/\sigma_0$; where $\sigma_0^2 = \langle \Psi^2 \rangle$ are defined as follows:

$$V_k(\nu) = \frac{1}{(2\pi)^{(k+1)/2}} \frac{\omega_2}{\omega_{2-k}\omega_k} \exp\left(-\frac{\nu^2}{2}\right) \left(\frac{\sigma_1}{\sqrt{2}\sigma_0}\right)^k \left[V_k^{(2)}(\nu)\sigma_0 + V_k^{(3)}(\nu)\sigma_0^2 + V_k^{(4)}(\nu)\sigma_0^3 + \dots \right]$$

$$V_k^{(2)}(\nu) = \left[\frac{1}{6} S^{(0)} H_{k+2}(\nu) + \frac{k}{3} S^{(1)} H_k(\nu) + \frac{k(k-1)}{6} S^{(2)} H_{k-2}(\nu) \right] \quad (3)$$

$$\sigma_j^2 = \frac{1}{4\pi} \sum_l (2l+1)[l(l+1)]^j C_l b_l^2 \equiv \sum_l (2l+1)[\sigma_j^2]_l \quad (4)$$

The constant ω_k introduced above is the volume of the unit sphere in k-dimension. $\omega_k = \frac{\pi^{k/2}}{\Gamma(k/2+1)}$ in 2D we will only need $\omega_0 = 1$, $\omega_1 = 2$ and $\omega_2 = \pi$. The lowest order Hermite polynomials $H_k(\nu)$ are listed below. The expression consists of two distinct contributions. The part which do not depend on the three different skewness parameters $S^{(0)}, S^{(1)}, S^{(2)}$ and signifies the MFs for a Gaussian random field. The other contribution $\delta V_k(\nu)$ represents the departure from the Gaussian statistics and depends on the generalized skewness parameters defined in Eq.(6) and Eq.(10).

$$\begin{aligned}
H_{-1}(\nu) &= \sqrt{\frac{\pi}{2}} \exp\left(\frac{\nu^2}{2}\right) \operatorname{erfc}\left(\frac{\nu}{\sqrt{2}}\right); \quad H_0(\nu) = 1, \quad H_1(\nu) = \nu, \\
H_2(\nu) &= \nu^2 - 1, \quad H_3(\nu) = \nu^3 - 3\nu, \quad H_4(\nu) = \nu^4 - 6\nu^2 + 3. \\
H_n(\nu) &= (-1)^n \exp\left(\frac{\nu^2}{2}\right) \frac{d}{d\nu^n} \exp\left(-\frac{\nu^2}{2}\right)
\end{aligned} \tag{5}$$

Various moments σ_j that appear in Eq.(4) can be expressed in terms of the power spectra \mathcal{C}_l and the observational beam b_l . The moment σ_0 is a spacial case which correspond to the variance. The quantities σ_1, σ_2 are natural generalizations of variance and they put more weights on higher harmonics. The variance that will mostly be used are $\sigma_0^2 = \langle \Psi^2 \rangle$ and $\sigma_1^2 = \langle (\nabla \Psi)^2 \rangle$.

The real space expressions for the triplets of skewness $S^{(i)}$ are given below. These are natural generalizations of the ordinary skewness S^0 that is used in many cosmological studies. They all are cubic statistics but are constructed from different cubic combinations.

$$S^{(0)} \equiv \frac{S^{(\Psi^3)}}{\sigma_0^4} = \frac{\langle \Psi^3 \rangle}{\sigma_0^4}; \quad S^{(1)} \equiv -\frac{3}{4} \frac{S^{(\Psi^2 \nabla^2 \Psi)}}{\sigma_0^2 \sigma_1^2} = -\frac{3}{4} \frac{\langle \Psi^2 \nabla^2 \Psi \rangle}{\sigma_0^2 \sigma_1^2}; \quad S^{(2)} \equiv \frac{S^{(\nabla \Psi \cdot \nabla \Psi \nabla^2 \Psi)}}{\sigma_1^4} = -3 \frac{\langle (\nabla \Psi) \cdot (\nabla \Psi) (\nabla^2 \Psi) \rangle}{\sigma_1^4} \tag{6}$$

The expressions in the harmonic domain are more useful in the context of CMB studies where we will be recovering them from masked sky using analytical tools that are commonly used for power spectrum analysis. The skewness parameter $S^{(1)}$ is constructed from the product field $[\Psi^2]$ and $[\nabla^2 \Psi]$, where as skewness parameter $S^{(2)}$ on the other hand relies on construction of $[\nabla \Psi \cdot \nabla \Psi]$ and $[\nabla^2 \Psi]$. By construction the skewness parameter $S^{(2)}$ has the highest weights on high l modes and $S^{(0)}$ has the lowest weights on high l modes. The expressions in terms of the bispectrum $B_{l_1 l_2 l_3}$ (see Eq.(11) for definition) take the following form (see e.g. Hikage et al. (2008)):

$$S^{(\Psi^3)} = \frac{1}{4\pi} \sum_{l_i} B_{l_1 l_2 l_3} I_{l_1 l_2 l_3} b_{l_1} b_{l_2} b_{l_3} \tag{7}$$

$$S^{(\Psi^2 \nabla^2 \Psi)} = -\frac{1}{12\pi} \sum_{l_i} \left[l_1(l_1 + 1) + l_2(l_2 + 1) + l_3(l_3 + 1) \right] B_{l_1 l_2 l_3} I_{l_1 l_2 l_3} b_{l_1} b_{l_2} b_{l_3} \tag{8}$$

$$S^{(\nabla \Psi \cdot \nabla \Psi \nabla^2 \Psi)} = \frac{1}{8\pi} \sum_{l_i} \left[[l_1(l_1 + 1) + l_2(l_2 + 1) - l_3(l_3 + 1)] l_3(l_3 + 1) + \text{cyc.perm.} \right] B_{l_1 l_2 l_3} I_{l_1 l_2 l_3} b_{l_1} b_{l_2} b_{l_3} \tag{9}$$

$$I_{l_1 l_2 l_3} = \sqrt{\frac{(2l_1 + 1)(2l_2 + 1)(2l_3 + 1)}{4\pi}} \begin{pmatrix} l_1 & l_2 & l_3 \\ 0 & 0 & 0 \end{pmatrix}. \tag{10}$$

We will use the same notation $b_{l_1 l_2 l_3}$ for the reduced bispectrum and the beam b_l . The number of subscripts however is enough to distinguish them.

The bispectrum $B_{l_1 l_2 l_3}$ used here defines the three-point correlation function in the harmonic domain. In general a reduced bispectrum $b_{l_1 l_2 l_3}$ is commonly used in certain situations which can directly be linked to the flat-sky expressions.

$$\langle a_{l_1 m_1} a_{l_2 m_2} a_{l_3 m_3} \rangle_c = \begin{pmatrix} l_1 & l_2 & l_3 \\ m_1 & m_2 & m_3 \end{pmatrix} B_{l_1 l_2 l_3}; \quad B_{l_1 l_2 l_3} = I_{l_1 l_2 l_3} b_{l_1 l_2 l_3} \tag{11}$$

The expressions for the MFs in Eq.(4) that we have discussed, depend on the one-point cumulants $S^{(i)}$. However it is possible to define power spectra associated with each of these skewness parameters following a procedure developed in Munshi & Heavens (2010). This will mean we can also associate a power spectrum with $V_k^{(3)}$ which will generalize the concept of MFs in a scale dependent way. The power spectrum that we associate with MFs will have the same correspondence with various skew-spectra $S_l^{(i)}$ that the MFs have with one-point cumulants or $S^{(0)}$. The power spectra such defined will however have more power to distinguish various models of non-Gaussianity. This is one of the main motivation behind generalizing the concept of MFs, which is a number, to a power spectrum.

The series expansion for the MFs can be extended beyond the level of the bispectrum. The next to the leading order corrections terms are related to trispectra of original fields and various derivatives constructed from the original field by using differential operations such as $[\nabla \cdot \nabla]$, $[\nabla^2]$. These corrections are however expected to be sub-dominant in the context of CMB studies for the entire range of angular scales being probed.

The results here correspond to temperature maps, which is a spin-0 object. It is possible to extend these results to the case of polarization analysis i.e. for spin-2 fields. Such results will also be context of weak lensing shear and flexions. A detailed analysis will be presented elsewhere.

3 THE TRIPLETS OF SKEW-SPECTRA AND LOWEST ORDER CORRECTIONS TO GAUSSIAN MFs

The skew-spectra are cubic statistics that are constructed by cross-correlating two different fields. One of the fields used is a composite field typically a product of two maps either in its original form or constructed by means of relevant differential operations. The second field will typically be a single field but may be constructed by applying various differential operators. All of these three skewness parameters contribute to the three MFs that we will consider in 2D.

The first of the skew-spectra was studied by (Cooray 2001) and later by Munshi & Heavens (2010) and is related to commonly used skewness. The skewness in this case is constructed by cross-correlating the squared map $\Psi^2(\hat{\Omega})$ with the original map $\Psi(\hat{\Omega})$. The second skew-spectrum is constructed by cross-correlating the squared map $[\Psi^2(\hat{\Omega})]$ against $[\nabla^2 \Psi(\hat{\Omega})]$. Analogously the third skew-spectrum represents the cross-spectra that can be constructed using $[\nabla \Psi(\hat{\Omega}) \cdot \nabla \Psi(\hat{\Omega})]$ and $[\nabla^2 \Psi(\hat{\Omega})]$ maps.

Local Model

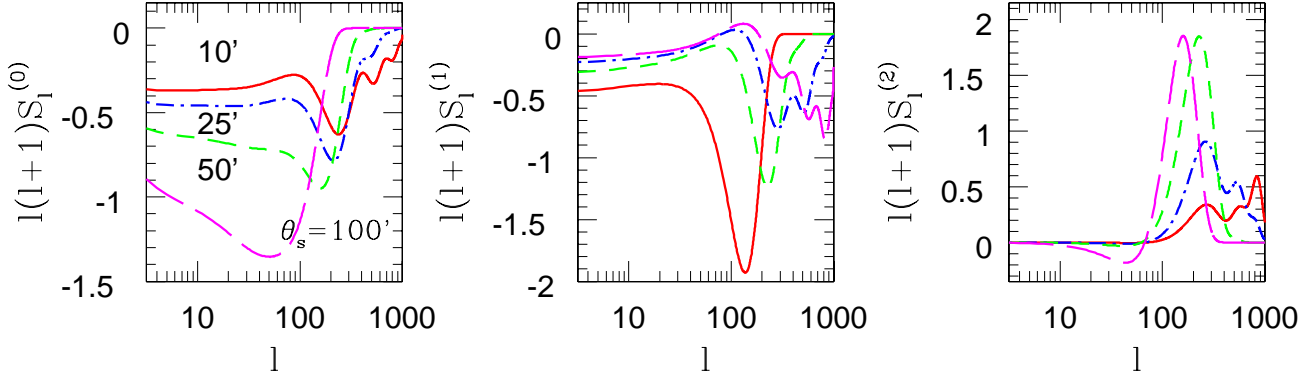


Figure 3. The skew-spectra $S_l^{(0)}$ (left-panel), $S_l^{(1)}$ (middle-panel) and $S_l^{(2)}$ (right-panel) are plotted for various smoothing beam (see Eq.(16)) as function of the harmonics l . The model for the primordial non-Gaussianity is assumed to be a local model for these plots Eq.(44). The underlying cosmology is assumed to be that of WMAP7. The three FWHM for the three beams considered are $\theta_s = 10'$ (solid), $25'$ (dot-dashed), $50'$ (small-dashed), $100'$ (long-dashed). The parameter f_{NL}^{loc} describing the normalization of local model of non-Gaussianity is set to unity $f_{NL}^{loc} = 1$. The resolution is set at $l_{max} = 1024$. To extract the skewness parameters we can use the relationship $S^i = \sum_l (2l+1) S_l^i$.

Equilateral Model

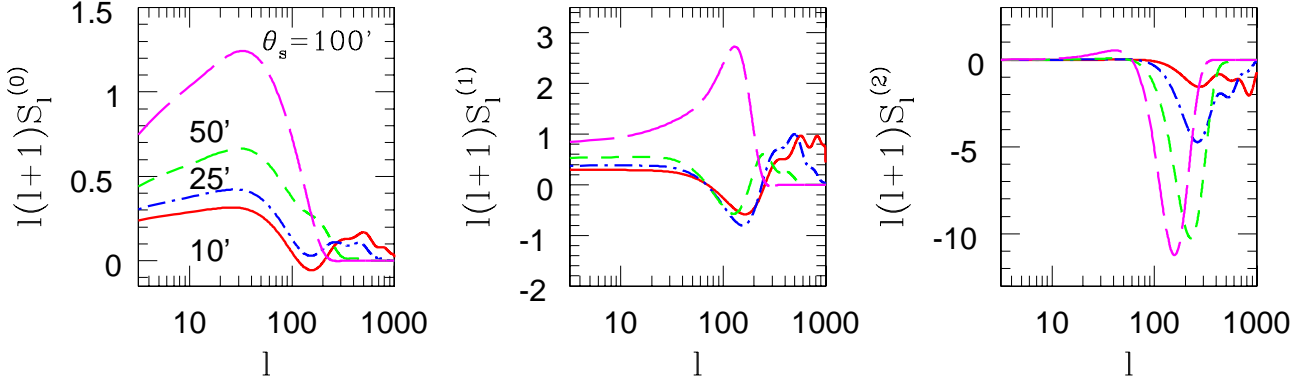


Figure 4. Same as previous figure but for the equilateral model of primordial non-Gaussianity as defined in Eq.(45). The choice of smoothing angular scales (beam) are same as previous figure. The normalization parameter for equilateral bispectrum f_{NL}^{equi} is set to unity $f_{NL}^{equi} = 1$. We consider three different beams as indicated $\theta_s = 10'$ (solid), $25'$ (dot-dashed), $50'$ (small-dashed), $100'$ (long-dashed). The shape of the two skew-spectra as derived from equilateral and local model are different and can be used to differentiate their contributions in real data.

$$S_l^{(0)} \equiv \frac{1}{4\pi\sigma_0^4} S_l^{(\Psi^2, \Psi)} \equiv \frac{1}{4\pi\sigma_0^4} \frac{1}{2l+1} \sum_m \text{Real}([\Psi]_{lm} [\Psi^2]_{lm}^*) = \frac{1}{4\pi\sigma_0^4} \sum_{l_1 l_2} B_{ll_1 l_2} J_{ll_1 l_2} b_{l_1} b_{l_2} \quad (12)$$

$$\begin{aligned} S_l^{(1)} &\equiv \frac{1}{16\pi\sigma_0^2\sigma_1^2} S_l^{(\Psi^2, \nabla\Psi)} \equiv \frac{1}{16\pi\sigma_0^2\sigma_1^2} \frac{1}{2l+1} \sum_m \text{Real}([\nabla^2\Psi]_{lm} [\Psi^2]_{lm}^*) \\ &= \frac{1}{16\pi\sigma_0^2\sigma_1^2} \sum_{l_i} \left[l(l+1) + l_1(l_1+1) + l_2(l_2+1) \right] B_{ll_1 l_2} J_{ll_1 l_2} b_{l_1} b_{l_2} b_{l_3} \end{aligned} \quad (13)$$

$$\begin{aligned} S_l^{(2)} &\equiv \frac{1}{8\pi\sigma_1^4} S_l^{(\nabla\Psi \cdot \nabla\Psi, \nabla^2\Psi)} \equiv \frac{1}{8\pi\sigma_1^4} \frac{1}{2l+1} \sum_m \text{Real}([\nabla\Psi \cdot \nabla\Psi]_{lm} [\nabla^2\Psi]_{lm}^*) \\ &= \frac{1}{8\pi\sigma_1^4} \sum_{l_i} \left[[l(l+1) + l_1(l_1+1) - l_2(l_2+1)] l_2(l_2+1) + \text{cyc.perm.} \right] B_{ll_1 l_2} J_{ll_1 l_2} b_{l_1} b_{l_2} b_{l_3} \end{aligned} \quad (14)$$

$$J_{l_1 l_2 l_3} \equiv \frac{I_{l_1 l_2 l_3}}{2l_3+1} = \sqrt{\frac{(2l_2+1)(2l_3+1)}{(2l_1+1)4\pi}} \begin{pmatrix} l_1 & l_2 & l_3 \\ 0 & 0 & 0 \end{pmatrix}. \quad (15)$$

$$S^{(i)} = \sum_l (2l+1) S_l^{(i)} \quad (16)$$

These set of equations constitute one of the main results in this paper. The matrices here denote Wigner-3j (3j) symbols, b_l represents the experimental beam $b_l = \exp \{-l(l+1)/2\sigma_b^2\}$ with $\sigma_b = \text{FWHM}/\sqrt{8 \ln 2}$ for a Gaussian beam. Each of these spectra probes the same bispectra $B_{l_1 l_2}$ with different weights for individual triplets of modes that specifies the bispectrum $(l, l_1 l_2)$. These triplets of modes specifies a triangle in the harmonic domain. The skew-spectra sums over all possible configuration of the bispectrum keeping one of its side l fixed. For each individual choice of l we can compute the skew-spectra $S_l^{(i)}$. The extraction of skew-spectra from data is relatively straight forward. It consists of construction the relevant maps in real space either by algebraic or differential operation and then cross-correlating them in the multipole space. The issues related to mask and noise will be dealt with in later sections. We will show that even in the presence of mask the computed skew spectra can be inverted to give a unbiased estimate of all-sky skew-spectra. The presence of noise will only affect the scatter. We have explicitly displayed the experimental beam b_l in all our expressions.

To derive the above expressions, we first express the spherical harmonic expansion of fields the $[\nabla^2 \Psi(\hat{\Omega})]$, $[\nabla \Psi(\hat{\Omega}) \cdot \nabla \Psi(\hat{\Omega})]$ and $[\Psi^2(\hat{\Omega})]$ in terms of the harmonics of the original fields Ψ_{lm} . These expressions involve the 3j functions as well as factors that depend on various l_i dependent weight factors.

$$\begin{aligned} [\nabla^2 \Psi(\hat{\Omega})]_{lm} &= \int d\hat{\Omega} Y_{lm}^*(\hat{\Omega}) [\nabla^2 \Psi(\hat{\Omega})] = -l(l+1) \Psi_{lm} \\ [\Psi^2(\hat{\Omega})]_{lm} &= \int d\hat{\Omega} Y_{lm}^*(\hat{\Omega}) [\Psi^2(\hat{\Omega})] = \sum_{l_i m_i} (-1)^m f_{l_1 m_1} \Psi_{l_2 m_2} I_{l_1 l_2 l} \begin{pmatrix} l_1 & l_2 & l \\ m_1 & m_2 & -m \end{pmatrix}. \\ [\nabla \Psi(\hat{\Omega}) \cdot \nabla \Psi(\hat{\Omega})]_{lm} &= \int d\hat{\Omega} Y_{lm}^*(\hat{\Omega}) [\nabla \Psi(\hat{\Omega}) \cdot \nabla \Psi(\hat{\Omega})] = \sum_{l_i m_i} \Psi_{l_1 m_1} \Psi_{l_2 m_2} \int d\hat{\Omega} Y_{lm}^*(\hat{\Omega}) [\nabla Y_{l_1 m_2}(\hat{\Omega}) \cdot \nabla Y_{l_2 m_2}(\hat{\Omega})] \end{aligned} \quad (17)$$

$$\begin{aligned} &= \frac{1}{3} \sum_{l_i m_i} [l_1(l_1+1) + l_2(l_2+1) - l(l+1)] \int d\hat{\Omega} Y_{lm}^*(\hat{\Omega}) Y_{l_1 m_1}(\hat{\Omega}) Y_{l_2 m_2}(\hat{\Omega}) \\ &= \frac{1}{3} \sum_{l_i m_i} (-1)^m [l_1(l_1+1) + l_2(l_2+1) - l(l+1)] \Psi_{l_1 m_1} \Psi_{l_2 m_2} I_{l_1 l_2 l} \begin{pmatrix} l_1 & l_2 & l \\ m_1 & m_2 & -m \end{pmatrix}. \end{aligned} \quad (18)$$

We can define the power spectrum associated with the MFs through the following third order expression:

$$V_k^{(3)} = \sum_l [V_k]_l (2l+1) = \frac{1}{6} \sum_l (2l+1) \left\{ S_l^{(0)} H(\nu) + \frac{k}{3} S_l^{(1)} H(\nu) + \frac{k(k-1)}{6} S_l^{(2)} H_{k-2}(\nu) + \dots \right\}. \quad (19)$$

The three skewness parameters defines the triplets of Minkowski Functional. At the level of two-point statistics, in harmonic domain we have three power-spectra associated with Minkowski-Functional $V_k^{(3)}$ that depend on the three skew-spectra we have defined. We will show later in this paper that the fourth order correction terms too have a similar form with an additional monopole contribution that can be computed from the lower order one-point terms such as the three skewness defined here. The result presented here is important and implies that we can study the contributions to each of the MFs $v_k(\nu)$ as a function of harmonic mode l . This is a especially significant result as various forms of non-Gaussianity will have different l dependence and hence they can potentially be distinguished. The ordinary MFs adds contributions from individual l modes and hence have less power in differentiating various contributing sources of non-Gaussianity. This is one of main motivations to extend the concept of MFs (single numbers) to one-dimensional objects similar to the power spectrum.

In Figure-2 we have plotted the variance parameters $[\sigma_0^2]_l$ and $[\sigma_1^2]_l$ for various smoothing beam (assumed Gaussian). The four different FWHM that are being considered are $\theta_s = 10', 25', 50'$ and $100'$ respectively. These parameters only depend on the underlying CMB power spectra and the beam. They are used as a normalization parameters while constructing the MFs from the generalized skewness parameters (see Eq.(10)). The specific model that was considered for this particular plot is called *local* model (defined in Eq.(44)). The skew-spectra that correspond to the other popular model for primordial bispectrum is known as *equilateral* model (see Eq.(45)). We plot the corresponding skew-spectra in Figure-4 as a function of angular harmonics l . The shape of the skew-spectra for various model can provide the necessary clues to the origin of primordial bispectra while analyzing CMB maps. In Figure-3 we have presented the three different skew-spectra defined here S_l as a function of the harmonics l . The skew-spectra for a generic bispectrum is defined in Eq.(12), Eq.(13) and in Eq.(15). The skew spectra are sensitive to the smoothing b_l moreover the skew-spectra at a given l depend on the bispectrum defined over the entire range of l being probed. The normalization parameters for these plots are set to be equal to unity; i.e. we take $f_{NL}^{loc} = 1$ and $f_{NL}^{equi} = 1$. The skew-spectra will scale linearly with these parameters.

The point sources act as a contamination in estimation of the primordial bispectrum. The skew-spectra for the point source are plotted in Figure-5. The specific model for the bispectrum that we consider is given in Eq.(51). The point sources are expected to dominate at higher l values. The normalization for the point source bispectrum is set by the parameter b_{PS} . In our study we take $b_{PS} = 10^{-27} \mu K^3$.

Next, we consider the higher order corrections to the MFs. These corrections takes contribution from the trispectrum. Corrections to the individual MFs can be expressed in terms of a set of four kurtosis which are formed from the trispectra. These kurtosis are one-point estimators and they differ the way sample the individual modes of the trispectra defined by the quadruplet of harmonic number $\{l_i\}; i = 1, 2, 3, 4$. These generalized kurtosis parameters (denoted by K^i) can be generalized to *kurt-spectra*, denoted as K_l^i , in a manner very similar to the skew-spectra. These kurt-spectra can be used to express the next order corrections to the power spectra associated with MFs.

4 THE QUADRUPLER OF KURT-SPECTRA AND NEXT TO LEADING ORDER CORRECTIONS

In a perturbative analysis, the leading order terms that signify non-Gaussianity in the analysis of MFs depend on the bispectrum or equivalently a set of skewness. The next to the leading order order correction terms depend on a set of *kurtosis* parameters $K^{(i)}$ that are fourth order statistics and are

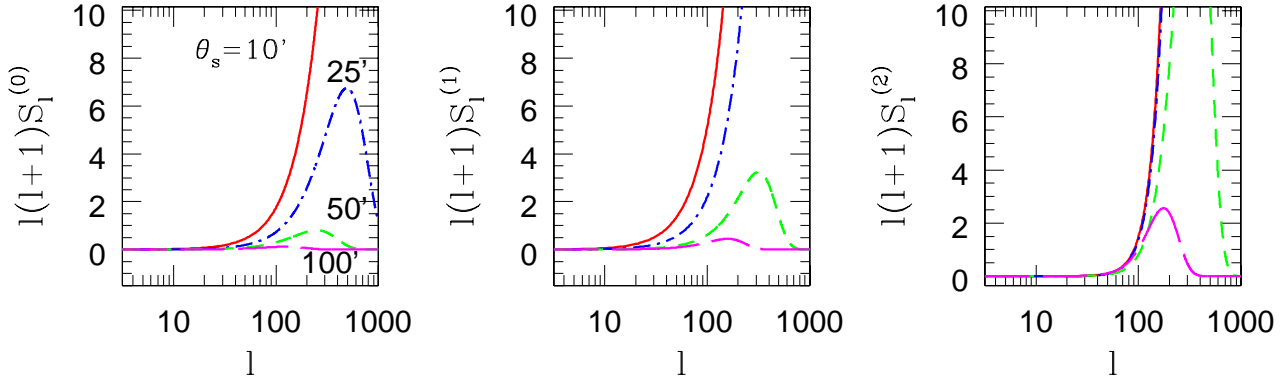


Figure 5. Same as previous figures but for point sources. For the point sources we have taken $b_{PS} = 10^{-27} \mu K^3$. The panels represent the three different skew-spectra $S_l^{(0)}$ (left-panel), $S_l^{(1)}$ (middle panel) and $S_l^{(2)}$ (right-panel) respectively. The skew-spectra are sensitive to the resolution of the maps being analyzed as they are integrated measures. This is related to the fact that its value at a specific harmonics l takes contribution from all possible modes, i.e. the entire range of l values. The point source contributions dominate the primordial non-Gaussianity at high l .

analogs of the skewness parameters $S^{(i)}$ we have defined above. In general the kurtosis parameters are collapsed fourth order one-point cumulants and probe the trispectrum with varying weights (see Munshi et al. (2010) for a more detailed discussion on fourth order one-point cumulants, their two-point counterparts or the cumulant correlators and related harmonic space description). The four different kurtosis parameters that are related to the MFs are a natural generalisation of the ordinary kurtosis $K^{(0)}$ which is routinely applied in many cosmological studies. We will denote these generalised kurtosis parameters by $K^{(i)}$; $i = 1, 2, 3$. These parameters are constructed from the derivative field of the original map $\Psi(\hat{\Omega})$ and its derivatives $[\nabla\Psi(\hat{\Omega})]$ and $[\nabla^2\Psi(\hat{\Omega})]$.

$$K^{(0)} \equiv \frac{1}{\sigma_0^6} K^{(\Psi^4)} = \frac{\langle \Psi^4 \rangle_c}{\sigma_0^6}; \quad K^{(1)} \equiv \frac{1}{\sigma_0^4 \sigma_1^2} K^{(\Psi^3 \nabla^2 \Psi)} = \frac{\langle \Psi^3 \nabla^2 \Psi \rangle_c}{\sigma_0^4 \sigma_1^2}; \quad (20)$$

$$K^{(2)} \equiv K^{(2a)} + K^{(2b)} \equiv \frac{1}{\sigma_0^2 \sigma_1^4} K^{(\Psi |\nabla\Psi|^2 \nabla^2 \Psi)} + \frac{1}{\sigma_0^2 \sigma_1^4} K^{(|\nabla\Psi|^4)} = \frac{\langle \Psi |\nabla\Psi|^2 (\nabla^2 \Psi) \rangle_c}{\sigma_0^2 \sigma_1^4} + \frac{\langle |\nabla\Psi|^4 \rangle_c}{\sigma_0^2 \sigma_1^4}; \quad (21)$$

$$K^{(3)} \equiv \frac{1}{2\sigma_0^2 \sigma_1^4} K^{(|\nabla\Psi|^4)} = \frac{\langle |\nabla\Psi|^4 \rangle_c}{2\sigma_0^2 \sigma_1^4}. \quad (22)$$

The subscript c correspond to the connected components which indicates that all Gaussian unconnected contributions are subtracted out, these include both noise as well as the signal contribution. The evaluation of these moments are relatively easy in real space for a pixelised map. It involves taking derivatives of beam smoothed maps. The corresponding power spectra associated with these fourth order moments are constructed by cross-correlating appropriate maps in the harmonic domain and are easy to implement numerically (Eq.(40) provides exact expressions for the corresponding power spectra or the kurt-spectra.).

The next to leading order corrections to the MFs involve these $K^{(i)}$ s as well as the product of two skewness parameters $S^{(i)}$ (i.e. the terms such as $[S^{(0)}]^2$, $[S^{(0)} S^{(1)}]$ or $[S^{(1)} S^{(2)}]$) defined previously in the context of leading order non-Gaussian terms (Matsubara 2010).

$$v_0^{(4)}(\nu) = \frac{[S^{(0)}]^2}{72} H_5(\nu) + \frac{K^{(0)}}{24} H_3(\nu); \quad v_1^{(4)}(\nu) = \frac{[S^{(0)}]^2}{72} H_6(\nu) + \left[\frac{K^{(0)} - S^{(0)} S^{(1)}}{24} \right] H_4(\nu) - \frac{1}{12} \left[K_1 + \frac{3}{8} [S^{(1)}]^2 \right] H_2(\nu) - \frac{1}{8} K^{(3)} \quad (23)$$

$$v_2^{(4)}(\nu) = \frac{[S^{(0)}]^2}{72} H_7(\nu) + \left[\frac{K^{(0)} - S^{(0)} S^{(1)}}{24} \right] H_5(\nu) - \frac{1}{6} \left[K^{(1)} + \frac{1}{2} S^{(0)} S^{(2)} \right] H_3(\nu) - \frac{1}{2} \left[K^{(2)} + \frac{1}{2} S^{(1)} S^{(2)} \right] H_1(\nu). \quad (24)$$

The analytical modelling of four-point correlation functions is most naturally done in the harmonic domain. They are described by the angular trispectrum $T_{l_3 l_4}^{l_1 l_2}(L)$ which is defined through the relation $\langle a_{l_1 m_1} a_{l_2 m_2} a_{l_3 m_3} a_{l_4 m_4} \rangle_c = \sum_L I_{l_1 l_2 L} I_{l_3 l_4 L} T_{l_3 l_4}^{l_1 l_2}(L)$. The trispectrum $T_{l_3 l_4}^{l_1 l_2}(l)$ is expressed in terms of the reduced trispectrum $P_{l_3 l_4}^{l_1 l_2}(l)$. Following expression was introduced by Hu (2001) and encodes all possible inherent symmetries.

$$T_{l_3 l_4}^{l_1 l_2}(l) = P_{l_3 l_4}^{l_1 l_2}(l) + (2l+1) \left[\sum_{l'} (-1)^{l_2+l_3} \left\{ \begin{matrix} l_1 & l_2 & l \\ l_4 & l_3 & l' \end{matrix} \right\} P_{l_2 l_4}^{l_1 l_3}(l') + \sum_{l'} (-1)^{L+L'} \left\{ \begin{matrix} l_1 & l_2 & l \\ l_3 & l_4 & l' \end{matrix} \right\} P_{l_3 l_2}^{l_1 l_4}(l') \right]. \quad (25)$$

The matrices in curly brackets represent 6j symbols which are defined using 3j symbols (see Edmonds (1968) for more detailed discussions). The entites $P_{l_3 l_4}^{l_1 l_2}(l)$ can be further decomposed in terms of the *reduced* trispectrum $\tau_{l_3 l_4}^{l_1 l_2}(l)$:

$$P_{l_3 l_4}^{l_1 l_2}(l) = \tau_{l_3 l_4}^{l_1 l_2}(l) + (-1)^{\Sigma_U} \tau_{l_3 l_4}^{l_2 l_1}(l) + (-1)^{\Sigma_L} \tau_{l_4 l_3}^{l_1 l_2}(l) + (-1)^{\Sigma_L + \Sigma_U} \tau_{l_4 l_3}^{l_2 l_1}(l); \quad \Sigma_L = l_1 + l_2 + L; \quad \Sigma_U = l_3 + l_4 + L. \quad (26)$$

Each individual model for primordial non-Gaussianity makes a specific prediction for the *reduced* trispectrum which can be used as a fingerprint to rule out many possibilities.

Next we will introduce three additional trispectra that are constructed using different weights to the original trispectra $T_{l_3 l_4}^{l_1 l_2}(L)$ and differ the way they weight various modes, that are specified by a particular choice of the quadruplet $\{l_i\}$.

$$[T^{(0)}]_{l_3 l_4}^{l_1 l_2}(L) = T_{l_3 l_4}^{l_1 l_2}(L); \quad [T^{(1)}]_{l_3 l_4}^{l_1 l_2}(L) = \frac{1}{4} [l_1(l_1 + 1) + l_2(l_2 + 1) + l_3(l_3 + 1) + l_4(l_4 + 1)] T_{l_3 l_4}^{l_1 l_2}(L); \quad (27)$$

$$[T^{(2)}]_{l_3 l_4}^{l_1 l_2}(L) = \frac{1}{4} [L(L + 1) - (l_1(l_1 + 1) + l_2(l_2 + 1))(l_3(l_3 + 1) + l_4(l_4 + 1))] T_{l_3 l_4}^{l_1 l_2}(L); \quad (28)$$

$$[T^{(3)}]_{l_3 l_4}^{l_1 l_2}(L) = \frac{1}{4} [(l_1(l_1 + 1) + l_2(l_2 + 1) - L(L + 1))(l_3(l_3 + 1) + l_4(l_4 + 1) - L(L + 1))] T_{l_3 l_4}^{l_1 l_2}(L). \quad (29)$$

The four generalised kurtosis and the related kurt-spectra we have defined above can now be expressed in terms of these generalised tri-spectra $T^{(i)}$ as follows:

$$K^{(i)} = \sum_{l_i} \sum_L [T^{(i)}]_{l_3 l_4}^{l_1 l_2}(L) I_{l_1 l_2 L} I_{l_3 l_4 L}; \quad K_l^{(i)} = \sum_{l_i} [T^{(i)}]_{l_3 l_4}^{l_1 l_2}(l) J_{l_1 l_2 l} J_{l_3 l_4 l}; \quad \sum_i (2l + 1) K_l^{(i)} = K^{(i)}. \quad (30)$$

The fourth order expressions for the power spectra associated with MFs $v_l^{(i)}$ can be obtained by replacing all one-point $K^{(i)}$ s with their two-point counterparts $K_l^{(i)}$ in Eq.(24). The contributions from the skewness parameters only contribute in the monopole terms. The extraction of the kurt-spectra in the presence of a mask can be carried out analogous to the skew-spectra.

On a different note, the power spectra associated with the kurtosis or kurt-spectra are discussed in detail for a scalar field (Munshi et al. 2010), two different types of kurt-spectra were introduced in the context of analysis of CMB Temperature maps. These two kurt-spectra $K_l^{(2,2)}$ and $K_l^{(3,1)}$ both samples the relevant trispectrum. The first of these is constructed from cross-correlating the squared map with itself and is denoted as $K_l^{(2,2)}$. The other kurt-spectra is constructed from cross-correlating a cubic map with the original map $K_l^{(3,1)}$. In general different set of maps can also be used to form squared and cubic combinations which will probe a mixed trispectra. In the present context we are interested in the spectra $K_l^{(2,2)}$ as the construction of $K_l^{(3,1)}$ will involve gradient maps and are more complicated to analyse in a coordinate independent way.

The physical meaning of these kurt-spectra can be understood more easily in the harmonic domain. As mentioned, each individual modes of the trispectra is characterized by a specific choice of set of modes l_i that defines it. These modes each constitute the sides of a quadrangle whose diagonal is specified by the quantum number l . The kurt-spectra that we have considered here take contributions from all possible configurations of the quadrangle while keeping its diagonal l fixed.

The estimation of the kurt-spectra from a real data is relatively easy and follows the same methodology as that of the skew-spectra. The first of these kurt-spectra $K^{(0)}$ is extracted by cross-correlating the squared field $\Psi^2(\hat{\Omega})$ with itself. The spectra $K^{(1)}$ is constructed by cross-correlating $\Psi^2(\hat{\Omega})$ against $\Psi \nabla^2 \Psi$. The other two kurt-spectra can likewise be constructed. In each such construction a scalar map from a product field is generated before it cross-correlated with another such map. The reason we have not constructed the other kurt-spectra namely $K_l^{(3,1)}$ is simply related to the fact that scalar maps are not possible for all such cubic combinations e.g. those involving gradient fields i.e. $\nabla \Psi$ in a coordinate independent way. However such constructions are indeed possible using the spinorial formalism.

The corrections to the power spectrum associated with the MFs now can be written in terms of the $K_l^{(i)}$, i.e. the kurt-spectra and the various Hermite polynomials as introduced above. The contributions that higher powers or lower order statistics such as skewness will only contribute to the monopole term for every MFs. However the higher multipoles will involve contribution from various Kurt-spectra as indicated. Different specific choice of Trispectra will therefore lead us to completely different power spectra associated with the MFs and can help to distinguish various models of non-Gaussianity.

5 ESTIMATORS AND THEIR COVARIANCE

The results derived above correspond to the all-sky and no-noise situation. However, in reality often we have to deal with issues that are related to the presence of a mask and (inhomogeneous) noise. To correct for the effect of a mask and the noise we will follow the Pseudo- C_ℓ (PCL) method devised by Hivon et al. (2001) for power spectrum analysis and was later developed by (Munshi et al. 2009) for analyzing the skew spectra as well as the kurt-spectrum (Munshi et al. 2010).

The partial sky coverage introduces mode-mode coupling in the harmonic domain. Individual masked harmonics become linear combinations of all-sky harmonics. The coefficients for this linear transformation depends on specific choice of masks through its harmonic coefficients. We will devise a method that can be used to correct for the mode-mode coupling. Our method is based on PCL approach which is often used in reconstructing unbiased power spectrum. If we have a generic field $A(\hat{\Omega})$ and $B(\hat{\Omega})$ we denote their harmonic decomposition in the presence of mask $w(\hat{\Omega})$ as \tilde{A}_{lm} and \tilde{B}_{lm} . Notice that the mask is completely general and our results do not depend on any specific symmetry requirements such as the azimuthal symmetry. The fields A and B may correspond to any of the fields we have considered above. In a generic situation A and B will denote composite fields and the harmonics A_{lm} and B_{lm} will correspond to any of the harmonics listed in Eq.(18).

$$\tilde{A}_{lm} = \int d\hat{\Omega} Y_{lm}^*(\hat{\Omega}) w(\hat{\Omega}) A(\hat{\Omega}); \quad \tilde{B}_{lm} = \int d\hat{\Omega} Y_{lm}^*(\hat{\Omega}) w(\hat{\Omega}) B(\hat{\Omega}) \quad (31)$$

$$\tilde{A}_{lm} = \sum_{l_i m_i} (-1)^m I_{l l_i l_2} \begin{pmatrix} l_1 & l_2 & l \\ m_1 & m_2 & -m \end{pmatrix} w_{l_1 m_1} A_{l_2 m_2}; \quad \tilde{B}_{lm} = \sum_{l_i m_i} (-1)^m I_{l l_i l_2} \begin{pmatrix} l_1 & l_2 & l \\ m_1 & m_2 & -m \end{pmatrix} w_{l_1 m_1} B_{l_2 m_2}. \quad (32)$$

The above expression relates the masked harmonics denoted by \tilde{A}_{lm} and \tilde{B}_{lm} with their all-sky counterparts A_{lm} and B_{lm} respectively. In their derivation we use the Gaunt integral to express the overlap integrals involving three spherical harmonics in terms of the $3j$ symbols (Edmonds 1968). The expressions also depend on the harmonics of the mask w_{lm} . If we now denote the (cross) power spectrum constructed from the masked harmonics and denote it by \tilde{S}_l and its all-sky counterpart by S_l we can write:

$$\tilde{S}_l^{A,B} = \frac{1}{2l+1} \sum_m \tilde{A}_{lm} \tilde{B}_{lm}^*; \quad \tilde{S}_l^{A,B} = \sum_{l'} M_{ll'} S_l^{A,B}; \quad M_{ll'} = \frac{1}{2l+1} \sum_{l''} I_{ll'l''}^2 |w_{l''}|^2; \quad \{A, B\} \in \{\Psi, \Psi^2, (\nabla\Psi \cdot \nabla\Psi), \nabla^2\Psi\}. \quad (33)$$

In above derivation we have used the orthogonality properties of the $3j$ symbols. It is interesting to notice that the *convolved* power spectrum estimated from the masked sky is a linear combination of all-sky spectra and depends only on the power spectra of the mask used. The linear transform is encoded in the mode-mode coupling matrix $M_{ll'}$ which is constructed from the knowledge of the power spectrum of the mask. In certain situations where the sky coverage is low the direct inversion of the mode mixing matrix M may not be possible due to its singularity and binning may be essential. based on these results it is possible to define an unbiased estimator that we denote by $\hat{S}_l^{A,B}$. The noise due to its Gaussian nature, do not contribute in these estimators which is remain unbiased. However presence of noise is felt due to increase in the scatter or covariance of these estimator which can be computed analytically:

$$\hat{S}_l^{A,B} = \sum_{l'} [M^{-1}]_{ll'} \tilde{S}_{l'}^{A,B}; \quad \langle \delta \hat{S}_l^{A,B} \delta \hat{S}_{l'}^{A,B} \rangle = \sum_{LL'} M_{lL}^{-1} \langle \delta \tilde{S}_L^{A,B} \delta \tilde{S}_{L'}^{A,B} \rangle M_{L'l'}^{-1}; \quad \langle \hat{S}_l^{A,B} \rangle = S_l^{A,B}; \quad \{A, B\} \in \{\Psi, \Psi^2, (\nabla\Psi \cdot \nabla\Psi), \nabla^2\Psi\}. \quad (34)$$

Notice that the mode coupling matrix M is independent of the particular choice of the skew-spectrum that we are interested. Hence the same coupling matrix can be used to extract the power spectrum associated with the MFs as the MFs are constructed from the linear combinations of generalized skew-spectra.

$$[\hat{V}_k^{(2)}]_l = \sum_{l'} [M^{-1}]_{ll'} [\tilde{V}_k^{(2)}]_{l'}; \quad \langle \delta \hat{V}_k^{(2)} \delta \hat{V}_{k'}^{(2)} \rangle = \sum_{LL'} M_{lL}^{-1} \langle \delta [\tilde{V}_k^{(2)}]_l \delta [\tilde{V}_{k'}^{(2)}]_{l'} \rangle M_{L'l'}^{-1} \quad (35)$$

In the perturbative limit where the MFs are computed using the analytical results in Eq.(4) the information content of MFs is same as that of the bispectrum. The three skewness parameters that were defined in Eq.(6) all probe the same bispectrum with varying weights.

The variance $\langle \delta S_l^{A,B} \delta S_{l'}^{A,B} \rangle$ of various estimators can be constructed using the following procedure:

$$\langle \delta S_l^{A,B} \delta S_{l'}^{A,B} \rangle = C_l^{A,A} C_{l'}^{B,B} + [S_l^{A,B}]^2 \quad (36)$$

$$C_l^{\nabla \cdot \nabla, \nabla \cdot \nabla} = \sum_{l'l''} C_{l'} C_{l''} [l_1(l_1+1) + l_2(l_2+1) - l(l+1)]^2 I_{ll'l''}^2; \quad C_l^{[\Psi^2, \Psi^2]} = \sum_{l'l''} C_{l'} C_{l''} I_{ll'l''}^2; \quad C_l^{[\nabla^2\Psi, \nabla^2\Psi]} = l^2(l+1)^2 C_l \quad (37)$$

The symbols $C_l^{A,A}$ denote the power spectrum of the fields $A(\hat{\Omega})$; $A(\hat{\Omega})$ is a generic field that are used for the construction of generalized skew-spectra. The derivation of the covariance depends on a Gaussian approximation i.e. we ignore higher order non-Gaussianity in the fields. C_l is the ordinary CMB power spectra it also includes the effect of instrumental noise $C_l = C_l^S + C_l^N$. For a survey with homogeneous noise, ignoring the effect of beam we can write $C_l^N = \Omega_p \sigma_N^2$ where Ω_p is the pixel area and σ_N is the noise variance. In a regime when noise contributions dominate the MFs can be approximated by a Gaussian approximation.

The estimators for various skew-spectra are expected to be correlated to a certain extent. These can be expressed using following expression:

$$\langle \delta S_l^{A_1, B_1} \delta S_{l'}^{A_2, B_2} \rangle = C_l^{A_1, A_2} C_{l'}^{B_1, B_2} + S_l^{A_1, B_2} S_{l'}^{A_2, B_1}; \quad \{A_1, B_1, A_2, B_2\} \in \{\Psi, \Psi^2, (\nabla\Psi \cdot \nabla\Psi), \nabla^2\Psi\} \quad (38)$$

The above results are sufficient to compute the lowest order corrections to MFs due to the presence of non-Gaussianity as well as the scatter in the estimates in the presence of realistic mask and noise.

However the above method is also applicable to compute the leading order corrections to these terms, i.e. the kurt-spectra. These can be estimated using the results in Eq.(22), e.g. to construct the first of these kurt-spectra we have to cross-correlate the squared field Ψ^2 with it itself. Other kurt-spectra are similarly constructed by cross-correlating quadratic constructs which involve the derivative fields (see Eq.(29) and Eq.(30)):

$$K_l^0 = \frac{1}{2l+1} \sum_m [\Psi^2]_{lm} [\Psi^2]_{lm}^*; \quad K_l^0 = \frac{1}{2l+1} \sum_m [\Psi^2]_{lm} [\Psi \nabla^2 \Psi]_{lm}^* \quad (39)$$

$$K_l^{2a} = \frac{1}{2l+1} \sum_m [\Psi^2]_{lm} [\nabla^2 \Psi]_{lm}^*; \quad K_l^{2b} = \frac{1}{2l+1} \sum_m [\Psi^2]_{lm} [\Psi \nabla^2 \Psi]_{lm}^*; \quad K_l^3 = \frac{1}{2l+1} \sum_m [|\nabla \Psi|^2]_{lm} [|\nabla \Psi|^2]_{lm}^*. \quad (40)$$

We have defined two different estimators K_l^{2a} and K_l^{2b} that can be jointly used to construct the kurt-spectra K_l^2 . To compute the Gaussian contributions equivalent estimators needs to be define that works with simulated Gaussian maps with same power spectrum. The resulting Gaussian estimates will have to be subtracted from the above estimates. Equivalently, the Gaussian components of the kurt-spectra can be computed from Eq.(29) by replacing the generic trispectra with its corresponding Gaussian counterpart $G_{l_3 l_4}^{l_1 l_2}(L)$ (see e.g. Hu (2000) and Hu (2001)):

$$G_{l_3 l_4}^{l_1 l_2}(L) = (-1)^{l_1+l_3} \sqrt{(2l_1+1)(2l_3+1)} C_{l_1} C_{l_3} \delta_{L0} \delta_{l_1 l_2} \delta_{l_2 l_3} + (2L+1) C_{l_1} C_{l_2} [(-1)^{l_2+l_3+L} \delta_{l_1 l_3} \delta_{l_2 l_4} + \delta_{l_1 l_4} \delta_{l_2 l_3}]. \quad (41)$$

where \mathcal{C}_l is the power spectrum including noise.

The treatment for the masked sky will follow in an exactly same manner. For individual $K_l^{(i)}$ the unbiased estimators can be recovered using exactly the same mode-coupling matrix $M_{ll'}$ introduced before in Eq.(34); we have for the masked kurt-spectra $\hat{K}_l^{(i)} = M_{ll'}^{-1} \tilde{K}_{l'}^{(i)}$. The auto- and the covariance of these estimators can also be estimated using obvious generalization of Eq.(34) and Eq.(38) respectively. However previous studies have concluded that for realistic values of f_{NL} the corrections terms that involve the kurt-spectra will be almost negligible.

6 MINKOWSKI FUNCTIONALS AND THE CMB SKY

The discussion so far has been completely generic and is applicable to arbitrary random 2D field on the surface of the sky. We will specialize the discussion in this section to the case of CMB sky. CMB observations are the cleanest probes of primordial non-Gaussianity. The angular multispectra for the temperature fluctuations sample the 3D multispectra of the inflationary potential.

Given a specific form for the primordial non-Gaussianity It is possible to compute the MFs for the observed temperature perturbations. The non-Gaussianity in the CMB sky can be a direct manifestation of the non-Gaussianity in the seed perturbations generated during the inflation. The non-Gaussianity in inflationary potential is most easily characterized in the Fourier domain. The decomposition provides 3D Fourier coefficients $\Phi(\mathbf{k})$ for the wave vector \mathbf{k} . The following expression links the curvature fluctuations in Fourier space generated during inflation $\Phi(\mathbf{k})$ with spherical harmonic coefficients of temperature anisotropy a_{lm} with the help of radiation transfer function $\Delta_l(k)$ for the temperature fluctuations (Wang & Kamionkowski 2000). The angular power spectrum for the temperature fluctuations $\mathcal{C}_l = \langle a_{lm} a_{lm}^* \rangle$ can be expressed in terms of the power spectrum of the 3D perturbations in the potential field $\langle \Phi(\mathbf{k}_1) \Phi(\mathbf{k}_2) \rangle = (2\pi)^3 \delta_{3D}(\mathbf{k}_1 + \mathbf{k}_2) P_\Phi(k_1)$.

$$a_{lm} = 4\pi(-i)^l \int \frac{d^3k}{(2\pi)^3} \Phi(k) \Delta_l(k) Y_{lm}(\hat{k}); \quad \mathcal{C}_l = \frac{2}{\pi} \int k^2 dk P_\Phi(k) \Delta_l^2(k). \quad (42)$$

A Gaussian sky can be described statistically just by its angular power spectrum \mathcal{C}_l . The lowest order departure from the Gaussianity is described in terms of the bispectrum angular bispectrum. The general form for the 3D bispectrum for the inflationary potential Φ is given as $B_\Phi(k_1, k_2, k_3) = (2\pi)^3 \delta_{3D}(\mathbf{k}_1 + \mathbf{k}_2 + \mathbf{k}_3) F_\Phi(k_1, k_2, k_3)$. In general translational invariance enforces the momentum conservation in the Fourier domain will introduce the factor $\delta_{3D}(\mathbf{k}_1 + \mathbf{k}_2 + \mathbf{k}_3)$ involving the 3D Dirac delta function δ_{3D} . The kernel $F_\Phi(k_1, k_2, k_3)$ therefore is the amplitude of the bispectrum associated with each triangular configurations involving the wave vectors k_i . Various early Universe scenarios differ, the way they specify $F_\Phi(k_1, k_2, k_3)$. The reduced angular bispectrum defined in Eq.(11) can be expressed in terms of $F_\Phi(k_1, k_2, k_3)$:

$$b_{l_1 l_2 l_3} = \left(\frac{2}{\pi}\right)^3 \int dr r^2 \int k_1^2 dk_1 j_{l_1}(k_1 r) \Delta_{l_1}(k_1 r) \int k_2^2 dk_2 j_{l_2}(k_2 r) \Delta_{l_2}(k_2 r) \int k_3^2 dk_3 j_{l_3}(k_3 r) \Delta_{l_3}(k_3 r) F_\Phi(k_1, k_2, k_3). \quad (43)$$

Models of inflation can largely be divided into two different categories. The first class of models is known as the local model(45) (Komatsu & Spergel 2001; Medeiros & Contaldi 2006; Creminelli 2003; Creminelli et al. 2006; Cabella et al. 2006; Liguori et al. 2007; Smith, Senatore & Zaldarriaga 2009). In these models the contribution to the bispectrum is maximum for the squeezed configurations i.e. when $k_1 \gg k_2, k_3$. The other main class of models are called equilateral models (Chen, Huang & Kachru 2006; Chen, Easther & Lim 2007). In these class of models the maximum contribution correspond to a configuration where all wave vectors have similar magnitudes $k_1 \sim k_2 \sim k_3$ i.e. a equilateral configuration of the triangle representing the bispectrum in the Fourier space. It is important to note that unlike the local model the equilateral model can *not* be represented by product of separable functions. However approximate separable forms do exist in the literature (Creminelli et al. 2006; Smith & Zaldarriaga 2006). We quote the results for the CMB non-Gaussianity that arise in the context of local or equilateral models (Komatsu & Spergel 2001).

$$b_{l_1 l_2 l_3}^{loc} = 2f_{NL} \int r^2 dr [\beta_{l_1}(r) \beta_{l_2}(r) \alpha_{l_3}(r) + \text{cyc.perm}] \quad (44)$$

$$b_{l_1 l_2 l_3}^{equi} = 6f_{NL}^{eq} \int r^2 dr [-\alpha_{l_1}(r) \beta_{l_2}(r) \beta_{l_3}(r) - 2\delta_{l_1}(r) \delta_{l_2}(r) \delta_{l_3}(r) + \beta_{l_1}(r) \gamma_{l_2}(r) \delta_{l_3}(r) + \text{cyc.perm.}]. \quad (45)$$

The following functions are useful in analytical expression for the bispectrum and trispectrum (Creminelli et al. 2006):

$$\alpha_l(r) = \frac{2}{\pi} \int k^2 dk P_\Phi(k) j_l(kr) \Delta_l(k); \quad \beta_l(r) = \frac{2}{\pi} \int k^2 dk P_\Phi(k) j_l(kr) \Delta_l(k); \quad (46)$$

$$\gamma_l(r) = \frac{2}{\pi} \int k^2 dk P_\Phi^{1/3}(k) j_l(kr) \Delta_l(k); \quad \delta_l(r) = \frac{2}{\pi} \int k^2 dk P_\Phi^{2/3}(k) j_l(kr) \Delta_l(k); \quad (47)$$

$$F_L(r_1, r_2) = \frac{2}{\pi} \int k^2 dk P_\Phi^{2/3}(k) j_l(kr_1) j_l(kr_2). \quad (48)$$

Here j_l is spherical Bessel function, Φ is the inflationary potential $\Delta_l(k)$ is the radiation transfer function which can be computed using the publicly available software such as CAMB³ or CMBFAST⁴. In addition to the bispectra the *reduced* CMB trispectrum in the local model can be expressed in terms of these functions as (Hu 2000, 2001; Komatsu & Spergel 2001; Kogo et al. 2006):

³ <http://camb.info/>

⁴ <http://www.cmbfast.org/>

$$\begin{aligned} \tau_{l_3 l_4}^{l_1 l_2}(L) = & 4f_{NL}^2 h_{l_1 l_2 L} h_{l_3 l_4 L} \int r_1^2 dr_1 \int r_2^2 dr_2 F_L(r_1, r_2) \alpha_{l_1}(r_1) \beta_{l_2}(r_1) \alpha_{l_3}(r_2) \beta_{l_4}(r_2); \\ & + g_{NL} h_{l_1 l_2 L} h_{l_3 l_4 L} \int r^2 dr \beta_{l_2}(r) \beta_{l_4}(r) [\mu_{l_1}(r) \beta_{l_3}(r) + \mu_{l_3}(r) \beta_{l_1}(r)]. \end{aligned} \quad (49)$$

For detailed discussions about various issues related to the symmetries and modeling of the CMB trispectrum see (Hu & Okamoto 2002; Hu 2000, 2001; Komatsu & Spergel 2001; Kogo et al. 2006).

In the limit of low multipole the perturbations are dominated by Sachs-Wolfe effect. In this regime the transfer function $\Delta_l(k)$ takes a simpler form; $\Delta(k) = 1/3j_l(kr_*)$. Here r_* denotes the time elapsed since cosmic recombination $= \eta_0 - \eta_{dec}$. The specific form for the reduced bispectrum $b_{l_1 l_2 l_3}$ and reduced $\tau_{l_3 l_4}^{l_1 l_2}(L)$ are completely specified by the angular power spectra C_l in this limit (Hu 2000, 2001; Komatsu & Spergel 2001; Kogo et al. 2006):

$$b_{l_1 l_2 l_3}^{SW} = -6f_{NL}(C_{l_1}C_{l_2} + C_{l_2}C_{l_3} + C_{l_3}C_{l_1}); \quad [\tau_{l_3 l_4}^{l_1 l_2}(L)]^{SW} = 9C_{l_2}C_{l_4}(4f_{NL}^2 C_L + g_{NL}(C_{l_1} + C_{l_3}))I_{l_1 l_2 L}I_{l_3 l_4 L}. \quad (50)$$

The MFs in this limiting case will therefore be completely specified by the angular power spectra. The fact that MFs can be specified completely by the bispectrum for arbitrary smoothing scales simply means that for local as well as equilateral models the parameter f_{NL} is sufficient to fully characterize the MFs.

The point sources too contribute to the CMB bispectrum. The point source bispectrum is given by:

$$b_{l_1 l_2 l_3} = b_{PS}. \quad (51)$$

The exact value of the amplitude b_{PS} depends on the limiting flux used in a specific survey. In our study we have taken $b_{PS} = 10^{-27} \mu K^3$. The results of our computations are plotted in Figure-(5). We have considered three different Gaussian beams as indicated $\theta_s = 10', 25', 50',$ and $100'$. At higher resolution l the point-source contribution will dominate primordial bispectrum. The skew-spectra S_l^2 which puts more weights on smaller angular scales are more dominated by point source contributions.

7 CONCLUSIONS

Different approaches are essential while testing non-Gaussianity as they all exploit different statistical characteristics. There is no unique approach that can be adopted to describe or parametrize non-Gaussianity in a complete manner. Testing of non-Gaussianity therefore must be done using a battery of complementary techniques. Each of these techniques has a unique response to the real world issues such as the sky-coverage and instrumental noise. Any robust detection therefore will have to involve a simultaneous cross-validation of results obtain from independent methods. The most common characterization of non-Gaussianity involves a study of the bi-spectrum which represents lowest order departure from Gaussianity. Higher order non-Gaussianity can be studied using its higher order analogs i.e. the multi-spectrum. In contrast the topological estimators that we have studied here carry information of all-orders though in a collapsed (one-point) form. Analytical results for MFs for a Gaussian field is well understood; which forms the basis of all non-Gaussianity studies (Tomita 1986). There has been several previous studies on extraction of the MFs from the CMB data that rely either on simplification of radiative transfer using the Sachs-Wolfe limit (see e.g. Hikage et al. (2006)) and using a perturbative approach based on a series expansion of the MFs that can be studied order by order (Matsubara 2003, 1994). The MFs have also been studied using elaborate computer intensive non-Gaussian simulations (Komatsu et al. 2003; Spergel et al. 2007). Most of these studies were done using a specific model for the non-Gaussianity namely the local model introduced here in Eq.(1) which is parametrized by the parameter f_{NL} .

One of the main difficulties faced by one-point estimators, which also include the MF based approaches, is their inability to differentiate various sources of non-Gaussianity. The one-point estimators all effectively compress all available information to a single number. This has the advantage of increasing the signal to noise ratio but it loses the ability to differentiate various sources of non-Gaussianity. In any study of primordial non-Gaussianity it is of the utmost importance to avoid any cross-contamination from secondary sources (see e.g. Goldberg & Spergel (1999a,b); Cooray & Hu (2000)). In recent studies involving MFs, certain levels of disagreement has been noticed with studies that use bi-spectrum to probe non-Gaussianity (see e.g. Hikage et al. (2006)). Given the MFs based approaches only directly probe the bispectra, as the contributions from the higher order multi-spectra are sub-dominant, it is important to understand various reasons of these disagreements.

Recently Munshi & Heavens (2010) have developed a new technique to study non-Gaussianity. Instead of one-point estimators, e.g. the skewness, their method relies on a spectrum or skew-spectrum which is the Fourier transform of two-point objects known as cumulant correlators. These skew-spectra do not compress the all available information from the study of a bi-spectrum to a single number and their shape can help to distinguish among various sources of non-Gaussianity. Exploiting the perturbative expansion of the MFs it is possible to show that in the leading order of non-Gaussianity, the MFs depend on three generalized skewness parameters. We extend the concept of the skew-spectra to the study of these MFs and introduce a generalized skew-spectrum associated with each of these skewness. This allows us to introduce a series of numbers associated with each of the MFs. We call these objects the power spectrum associated with MFs. The advantage of cross-checking the contributions to MFs using the skew-spectra is they provide a method to test any contamination from sources which are simply cross-contaminants from secondaries or foregrounds. The two methods that compute the MFs should provide identical results. The method based on the skew-spectra are simpler to implement once the derivative fields are constructed. These methods are similar to moment based approaches for studying non-Gaussianity and hence can provide valuable basis for cross-comparison. We have shown that this can be implemented in a model independent way. Our method is based on a Pseudo- C_l approach and can handle arbitrary sky coverage and inhomogeneous noise distributions. The PCL approach is well understood in the context of power spectrum studies and its variance or scatter can be computed analytically. We provide generic analytical results for computation of scatter around the individual estimates. It is possible indeed to go beyond the lowest level in non-Gaussianity. However, it is expected that such correction will be sub dominant at least in the context of CMB data analysis.

Nevertheless we include the spectrum associated with the next order correction terms that were introduced by (Matsubara 2010). These terms represent kurtosis and the corresponding spectra are known as kurt-spectra. In their study (Munshi et al. 2009) introduced two set of kurt-spectra. Adopting their method we show that generic two-to-two kurt-spectra can be extracted from the data without introducing any additional complication. To summarize:

- In the context of CMB, the study of MFs is equivalent to the study of bispectrum.
- Higher order terms which depend on trispectrum make negligible contributions.
- However the MFs do not probe the full bispectrum but only weighted sums of modes or the three *generalised* skewness parameters.
- We have defined three generalized skew-spectra associated with each of these skewness parameters.
- Study of these skew-spectra can replace the study of MFs.
- The skew-spectra can all be probed for arbitrary mask and noise.
- The unbiased estimators can be constructed which can work in the presence of partial sky coverage.
- Their variance can also be computed *analytically* there by avoiding the use of non-Gaussian simulations completely.
- The MFs can be constructed from the knowledge of generalized skew-spectra and can be compared with the results from real space analysis.
- Additional skew-spectra can be constructed using various derivative fields constructed from the original field and can provide additional cross-checks or even help to separate various components of non-Gaussianity.
- Generalized skew-spectra can be used to separate individual components of NGs.

The approach we have developed here to study MFs in this paper will be most useful in case of weak lensing studies where real space analysis is difficult because of complex survey geometry. A detailed analysis will be presented elsewhere.

The generic results derived here will also be applicable to other areas which include analysis of redshift surveys (3D) or projected surveys (2D) that include weak lensing surveys or SZ surveys. Results of detailed analysis will be presented elsewhere (Munshi et al. 2010 in preparation). It is however important to keep in mind that unlike the other optimized estimators of f_{NL} based on bispectrum, the MFs are *sub-optimal* in nature.

In this paper we have concentrated mainly on all-sky expressions that involve expansion of relevant fields using spherical harmonics. In certain situations the flat-sky results may be more directly relevant. The flat sky approximations can be recovered by replacing the spherical harmonics $Y_{lm}(\theta, \phi) \approx (-1)^m \sqrt{\frac{2l+1}{4\pi}} J_m[(l + \frac{1}{2})\theta] \exp(im\phi)$. These results will be valid for high $l \gg 1$. Typically these will result in expressing the flat sky multi-spectra in terms of their all-sky counterparts i.e. $C_l \approx \mathcal{C}(l + \frac{1}{2})$ for power spectrum and $\mathcal{B}_{l_1 l_2 l_3} \approx I_{l_1 l_2 l_3} \mathcal{B}(l_1 + \frac{1}{2}, l_2 + \frac{1}{2}, l_3 + \frac{1}{2})$ for the bispectrum and an analogous relation holds at the level of trispectrum.

8 ACKNOWLEDGEMENTS

DM acknowledges support from STFC standard grant ST/G002231/1 at School of Physics and Astronomy at Cardiff University where this work was completed. AC and JS are supported by nsf-ast0645427 and NASA NNX10AD42G. DM acknowledges useful discussions with Geraint Pratten and Peter Coles.

REFERENCES

- Acquaviva V., Bartolo N., Matarrese S., Riotto A., 2003, Nucl. Phys. B667, 119
Alishahiha M., Silverstein E., Tong T., 2004, Phys. Rev. D70, 123505
Arkani-Hamed N., Creminelli P., Mukohyama S., Zaldarriaga M., 2004, JCAP0404:001
Babich D., 2005, Phys. Rev. D72, 043003
Babich D., Pierpaoli E., 2008, Phys. Rev. D77, 123011
Babich D. & Zaldarriaga M., 2004, Phys. Rev. D70, 083005
Babich D., Creminelli P., Zaldarriaga M., 2004, JCAP, 8, 9
Bartolo N., Matarrese S., Riotto A., 2006, JCAP, 06, 024
Bartolo N., Komatsu E., Matarrese S., Riotto A., 2004, Phys.Rept. 402, 103
Buchbinder E.I., Khoury J., Ovrut B.A., 2008, Phys.Rev.Lett.100:171302
Cabella P., Hansen F.K., Liguori M., Marinucci D., Matarrese S., Moscardini L., Vittorio N., 2006, MNRAS, 369, 819
Castro P., 2004, Phys. Rev. D67, 044039 (erratum D70, 049902)
Chen X., Huang M., Kachru S., Shiu G., 2006, hep-th/0605045
Chen X., Easther R., Lim E.A., 2007, JCAP, 0706:023
Chen G., Szapudi I., 2006, Astrophys.J.647:L87-L90
Cheung C., Creminelli P., Fitzpatrick A.L., Kaplan J., Senatore L., 2008, JHEP, 0803, 014
Cooray A.R., Hu W., 2000, ApJ, 534, 533-550
Cooray A., 2001, PhRvD, 64, 043516
Creminelli P., 2003, JCAP 0310, 003
Creminelli P., Nicolis A., Senatore L., Tegmark M., Zaldarriaga M., 2006, JCAP, 5, 4
Creminelli P., Senatore L., Zaldarriaga M., Tegmark M., 2007, JCAP, 3, 5
Creminelli P., Senatore L., Zaldarriaga M., 2007, JCAP, 3, 19
Edmonds, A.R., Angular Momentum in Quantum Mechanics, 2nd ed. rev. printing. Princeton, NJ:Princeton University Press, 1968.
Eriksen H.K., Novikov D.I., Lilje P.B., Banday A.J., Gorski K.M., 2004, ApJ, 612,64
Falk T., Madden R., Olive K.A., Srednicki M., 1993, Phys. Lett. B318, 354

- Gangui A., Lucchin F., Matarrese S., Mollerach S., 1994, ApJ, 430, 447
- Goldberg D.M., Spergel D.N., Phys.Rev. D59 (1999a) 103001
- Goldberg D.M., Spergel D.N., 1999b, Phys. Rev. D59, 103002
- Gupta S., Berera A., Heavens A.F., Matarrese S., 2002, Phys.Rev. D66, 043510
- Hadwiger H. 1959, Normale Koper im Euclidschen raum und ihre topologischen and metrischen Eigenschaften, Math Z., 71, 124
- Heavens A.F., 1998, MNRAS, 299, 805
- Hikage C., Matsubara T., Coles P., Liguori M., Hansen F.K., Matarrese S. 2008, MNRAS,389,1439
- Hikage C., Coles P., Grossi M., Moscardini L., Dolag K., Branchini L., Matarrese S. 2008, MNRAS,385,1513
- Hikage C., Komatsu E., Matsubara T., 2006, ApJ., 653, 11
- Hikage C., Taruya A., Suto Y., 2003, Publ.Astron.Soc.Jap, 55, 335
- Hikage C., et al. Publ.Astron.Soc.Jap. 54 (2002) 707
- Hikage C., et al. Publ.Astron.Soc.Jap. 55 (2003) 911
- Hivon E. et al., 2001, ApJ, 567, 2.
- Hu W., 2000, PhRvD, 62, 043007
- Hu W., 2001, PhRvD, 64, 083005
- Hu W., Okamoto T., 2002, ApJ, 574, 566
- Kogo N., Komatsu E. Phys.Rev. 2006, D73, 083007
- Komatsu E., Spergel D. N., 2001, Phys. Rev. D63, 3002
- Komatsu E., Spergel D. N., Wandelt B. D., 2005, ApJ, 634, 14
- Komatsu E., Wandelt B. D., Spergel D. N., Banday A. J., Górski K. M., 2002, ApJ, 566, 19
- Komatsu E., et al., 2003, ApJS, 148, 119
- Koyama K., Mizuno S., Vernizzi F., Wands D., 2007, JCAP 0711:024
- Larson et al. 2010, arXiv1001.4635
- Liguori M. & Riotto A., 2008, Phys. Rev.D78:123004
- Liguori M., Yadav A., Hansen F. K., Komatsu E., Matarrese S., Wandelt B., 2007, PhRvD, 76, 105016
- Linde A. D., Mukhanov V. F., (1997), Phys. Rev. D **56**, 535
- Lyth D.H., Ungarelli C., Wands D., 2003, Phys. Rev. D67, 023503
- Maldacena J.M., 2003, JHEP, 05, 013
- Matsubata T., 2010, Phys.Rev.D, 81, 083505
- Matsubara, T, 2003, ApJ, 584, 1
- Matsubara T., Jain B., 2001, ApJ, 552, L89.
- Matsubara T., 1994, ApJ, 434, L43
- Mecke K.R., Buchert T. & Wagner H., 1994, A&A, 288, 697
- Medeiros J., Contaldi C.R, 2006, MNRAS, 367, 39
- Moss I., Xiong C., 2007, JCAP, 0704, 007
- Munshi et al., arXiv:0907.3229
- Munshi et al., arXiv:0910.3693, MNRAS in press.
- Munshi D. Heavens A. 2010, MNRAS, 401, 2406
- Munshi D., Heavens A., Cooray A., Smidt J., Coles P., Serra P., 2009, arXiv:0910.3693 MNRAS in press.
- Munshi D., Souradeep, T., Starobinsky, Alexei A., 1995, ApJ, 454, 552
- Natoli et al. arXiv:0905.4301
- Novikov D., Schmalzing J., Mukhanov V.F., 2000, A&A 364, 17
- Park C. et al. ,2005, ApJ.633,11
- Salopek D. S., Bond J. R., 1990, PhRvD, 42, 3936
- Salopek D. S., Bond J. R., 1991, PhRvD, 43, 1005
- Santos M.G. et al., 2003, MNRAS, 341, 623
- Schmalzing J. & Buchert T. 1997, ApJ, 482, L1
- Schmalzing J. & Górski K.M. 1998, MNRAS, 297, 355
- Schmalzing J.,Takada M., Futamase T., 2000, ApJ, 544, L83, 2000
- Serra P., Cooray A., 2008, Phys.Rev.D77:107305
- Smith K.M., Zahn O., Dore O., 2007, Phys. Rev. D76:043510
- Smith K. M., Zaldarriaga M., 2006, arXiv:astro-ph/0612571
- Smith K.M., Senatore L., Zaldarriaga M., 2009, arXiv:0901.2572
- Spergel D.N., David M. Goldberg D. M., 1999a, Phys.Rev. D59, 103001
- Spergel D.N., David M. Goldberg D. M., 1999b, Phys.Rev. D59, 103002
- Spergel D.N. et al., 2007, ApJS, 170, 377
- Tauber et al, 2010, A&A, 520,1
- Taruya A., Takada M., Hamana T., Kayo I., Futamase T., 2002, ApJ, 571,638.
- Tomita H., 1986, Progr.Theor.Phys, 76, 952
- Verde L., Wang L., Heavens A., Kamionkowski M. Mon.Not.Roy.Astron.Soc. 313 (2000) L141-L147
- Verde L., Spergel D.N., 2002, Phys. Rev. D65, 043007
- Wang L., Kamionkowski M., 2001, Phys. Rev. D61, 3504

Winitizki S., Kosowsky A., 1998, *New. Astron.*, 3, 75

Yadav A. P. S., Wandelt B. D., 2008, *PhRvL*, 100, 181301

Yadav A. P. S., Komatsu E., Wandelt B. D., Liguori M., Hansen F. K., Matarrese S., 2008, *ApJ*, 678, 578

Yadav A. P. S., Komatsu E., Wandelt B. D., 2007, *ApJ*, 664, 680